Turbulent flows in a spiral double-pipe heat exchanger

Optimal performance conditions using an enhanced genetic algorithm

Zhe Tian
School of Engineering, Ocean University of China, Qingdao, China

Ali Abdollahi and Mahmoud Shariati
Department of Mechanical Engineering, Najafabad Branch, Islamic Azad University, Najafabad, Iran

Atefeh Amindoust
Department of Industrial Engineering, Najafabad Branch, Islamic Azad University, Najafabad, Iran

Hossein Arasteh
Department of Mechanical Engineering, Isfahan University of Technology, Isfahan, Iran

Arash Karimipour
Department of Mechanical Engineering, Najafabad Branch, Islamic Azad University, Najafabad, Iran, and

Marjan Goodarzi and Quang-Vu Bach
Sustainable Management of Natural Resources and Environment Research Group, Faculty of Environment and Labour Safety, Ton Duc Thang University, Ho Chi Minh City, Vietnam

Received 3 April 2019
Revised 20 July 2019
26 July 2019
Accepted 26 July 2019

Abstract

Purpose – This paper aims to study the fluid flow and heat transfer through a spiral double-pipe heat exchanger. Nowadays using spiral double-pipe heat exchangers has become popular in different industrial segments due to its complex and spiral structure, which causes an enhancement in heat transfer.

Design/methodology/approach – In these heat exchangers, by converting the fluid motion to the secondary motion, the heat transfer coefficient is greater than that of the straight double-pipe heat exchangers and cause increased heat transfer between fluids.

Findings – The present study, by using the Fluent software and nanofluid heat transfer simulation in a spiral double-tube heat exchanger, investigates the effects of operating parameters including fluid inlet velocity, volume fraction of nanoparticles, type of nanoparticles and fluid inlet temperature on heat transfer efficiency.

Originality/value – After presenting the results derived from the fluid numerical simulation and finding the optimal performance conditions using a genetic algorithm, it was found that water–Al_2O_3 and

The first author wants to acknowledge the following grants: NSFC (51709244), Taishan Scholar (tsqn201812025) and Fundamental Research Funds for the Central Universities (201941008).

International Journal of Numerical Methods for Heat & Fluid Flow
Vol. 30 No. 1, 2020
pp. 39-53

0961-5539
DOI 10.1108/HFF-04-2019-0287

water–SiO_2 nanofluids are the best choices for the Reynolds numbers ranging from 10,551 to 17,220 and 17,220 to 31,910, respectively.

Keywords Nanofluid, Optimization, Turbulent flow, Genetic algorithm, Heat exchanger

Paper type Research paper

Nomenclature

C_p = Specific heat transfer [J/kg.K];
f = Friction coefficient;
k = Thermal conductivity [W/m.K];
Nu = Nusselt number;
Re = Reynolds number;
U = Velocity in x-direction [m/s];
v = Velocity in y-direction [m/s]; and
w = Velocity in z-direction [m/s].

Greek symbols
ϑ = Kinematic viscosity [m^2/s];
μ = Dynamic viscosity [kg/m.s];
ρ = Fluid density [kg/m^3]; and
ϕ = Nanoparticles volume fraction.

Subscripts
f = Fluid;
nf = Nanofluid; and
s = Solid.

1. Introduction

Today, heat exchangers are playing a vital role in the industry with a wide application in refineries, chemical and food industries, air conditioning systems, cryogenic processes, waste heat recovery, etc. This equipment creates a high ratio of surface area to volume unit. In some studies, pipes are spiral (in the form of a spring), which create a centrifugal force in them (Chingulpitak and Wongwises, 2011; Zhao *et al.*, 2011). The secondary flow increases the heat transfer rate by decreasing the temperature differences. Therefore, in the heat transfer phenomenon, another displacement perpendicular to the flow is generated, which does not exist in the common devices. Figure 1 shows the schematic view of the spiral pipe structure and the secondary flow performance have been shown.

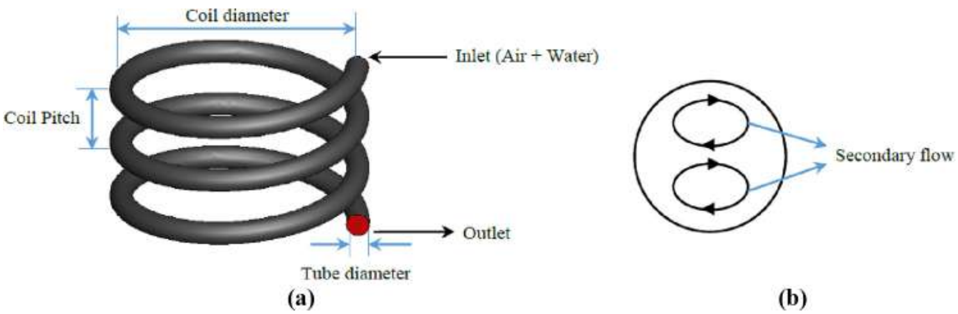

Figure 1.
(a) A general structure of a spiral pipe and (b) the secondary flow effect

Lots of studies have been done around the hydrodynamic and thermal properties of spiral pipes (Berger *et al.*, 1983; Naphon and Wongwises, 2006; Dravid *et al.*, 1971). Kurnia *et al.* (2011a) simulated the spiral pipes with a non-circular cross-sectional shape. These researchers, in another study, examined the heat transfer performance in cooling channels with different designs (Kurnia *et al.*, 2011b). In their study, the channel designs were parallel, wave, snake, fin diagonal and spiral tubes, and their research showed that spiral tubes have larger heat transfer. Naphon and Wongwises (2002) investigated the exclusive positive effects of heat transfer and fluid flow in horizontal pipes. In addition, the increase in heat transfer in the spiral coil is greater than the straight pipe. They investigated the properties of a spiral coil flow through the experimental and numerical methods.

Pawar (2013) made experimental studies concerned steady and unsteady supposed problems. Paisarn and Jamnean (2006) presented an article in the bending pipes. They showed that heat pipes worked better by some supposed heat transfer techniques for a specific heat transfer. Jang Yang (2012) investigated the spiral heat exchanger for different values of Re. In this experiment, the effect of Darcy friction and conductive heat transfer coefficient were measured from radial flow, which radial flow and screw flow were correlated to air and water, respectively. Two correlations were proposed, one for the Darcy friction coefficient and another for the Nusselt number. Salimpour (2009) studied a shell and tube heat exchanger with spiral tubes experimentally. They considered the viscosity, thermal conductivity, specific thermal capacity and density of the working fluid inside the tube as a function of temperature.

On the other hand, a lot of works reported the effects of different nanoparticles in heat exchangers so far. For example, the numerical simulation of flow and laminar convection in the space between the square channel and the solid pipe located in the center of it by Kalteh *et al.* (2011) can be pointed out. They used the Fluent software to perform numerical simulations and used a computer code developed by the user. The numerical simulation results showed suitable consistency with numerical data of pure water. Also, the results showed that by increasing the volumetric concentration of nanoparticles and decreasing the diameter of the nanoparticles, the heat transfer was improved. Moreover, they showed that concentration and the diameter of the larger nanoparticles would increase the friction coefficient. In another work, Kahani *et al.* (2013) studied the use of nanofluids in spiral coils experimentally. They stated that due to the bending of the coils, there was a significant increase in the amount of heat transfer and pressure drop. Saeedan *et al.* (2016) investigated modeling the computational fluid dynamics along with the neural network of a two-pipe heat exchanger with helix blades and the effect of different nanoparticles such as copper, copper oxide and carbon in various volume fractions. The modeling was carried out in single phase and three-dimensional conditions and the results showed that increasing the volume fraction of copper and copper oxide nanoparticles increases Nusselt number. Finally, with the aid of simulation results, a model was used to predict the Nusselt number and pressure drop in the heat exchanger, and the effect of parameters such as the Reynolds number, the volume fraction of nanoparticles and the type of nanoparticles in the neural network model was applied. In Maakoul *et al.* (2017), studied a double-pipe heat exchanger with helix-type buffers numerically. In their simulation, they used a three-dimensional model of computational fluid dynamics and Fluent software. The model was a single-phase model and they investigated the fluid flow in the circular section, the heat transfer coefficient, and the fluid pressure drop. In the following, a turbulent hydrodynamic and heat transfer of a turbulent flow through a spiral double-pipe heat exchanger is investigated. Moreover, the enhanced genetic algorithm of Pareto graph is used to optimize the heat transfer rate.

2. Mathematical modeling and numerical simulation process

Due to the very complex geometric nature of the heat transfer phenomenon in the two spiral tube heat exchangers, analytical solving is impossible. In addition, the limitations of our laboratory resources lead us to the use of numerical solutions. Different methods for solving equations are used in computational fluid dynamics, which due to the use of Fluent commercial software, in this study the finite volume method has been used. In this method, with the discretization of the equations in the levels of control volumes, we arrive at a system of algebraic equations, which the main purpose is to solve this system.

2.1 Governing equations

The general form of the heat transfer equations is as follows:

$$\nabla . (\rho \Phi u) = \nabla . (\Gamma \nabla \Phi) + S_{\Phi} \tag{1}$$

Which the main equations can be obtained by replacing Φ with the following equations.

"$\Phi = 1$" results in the continuity equation, "$\Phi = u$" results in the x-momentum equation, "$\Phi = v$" results in the y-momentum equation, "$\Phi = w$" results in the *z*- momentum equation, and "$\Phi = E_{(\rho,T)}$" results in the energy *equation*.

2.2 Model geometry

The created grid for simulation is shown in Figure 2. Due to the fact that the pipe walls are exposed to heat flux, the created grid near the walls are smaller to increase the accuracy of the calculations. As hexagonal cells in meshing have a high capacity at high computational speed and convergence, these kind of mesh is used in this study. In the mesh production, it should be noted that as the surrounding areas of the pipe contain more intense temperature and velocity gradients, an intensive mesh with smaller cells is needed at these areas. For this purpose, at the whole volume pertain to the external surfaces of the pipes, the mesh element size is fixed at 2 μm while this size is fixed at 3 μm at the internal surfaces of the pipe shell.

The simulations are performed for a spiral pipe with the inner diameter of inner pipe equal to 4.75 mm and the inner diameter of outer pipe equal to 6.35 mm. Other geometric characteristics are shown in Table I.

To ensure about the grid independency of obtained results, four different grids are produced. The heat transfer coefficient of these models are compared in Table II. According to our results, increasing the distance between knots more than 2 μm does not change the heat transfer coefficient substantially. Therefore, fine grid with 1,239,300 elements is chosen for our further simulations.

2.3 Thermo-physical properties of nanofluid

The metal oxide types of nanofluids with nanoparticles of Al_2O_3, SiO_2 and CuO, which their thermo-physical properties are provided in Table III.

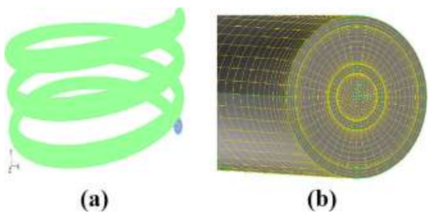

Figure 2.
(a) The schematic of the present study and its computational domain and (b) the generated mesh

The nanofluid density (Kahani *et al.*, 2013):

$$\rho_{nf} = (1-\phi)\rho_f + \phi\,\rho_{nf} \tag{2}$$

where at this equation, ρ_f is the base fluid density based on temperature and ρ_{nf} is the density of solid nanoparticles.

The nanofluid thermal conductivity (Saeedan *et al.*, 2016; Maakoul *et al.*, 2017):

$$(\rho C_p)_{nf} = (1-\phi)(\rho C_p)_f + \phi\,(\rho C_p)_{np} \tag{3}$$

$$k_{eff} = k_{static} + k_{Brownian} \tag{4}$$

$$k_{static} = k_f\left[\frac{(k_{np}+2k_f) - 2\phi\,(k_f - k_{np})}{(k_{np}+2k_f) + \phi\,(k_f - k_{np})}\right] \tag{5}$$

$$k_{Brownian} = 5\times10^4\,\beta\,\phi\,\rho_f C_{pf}\sqrt{\frac{KT}{2}}f(T,\phi) \tag{6}$$

where K is the Boltzman constant and is equal to 1.3807×10^{-23} J/K. Also, the refined equations by Das *et al.* is as follows:

$$f(T,\phi) = \left(2.8217\times10^{-2}\phi + 3.917\times10^{-3}\right)\left(\frac{T}{273.15}\right) + \left(-3.0669\times10^{-2}\phi - 3.91123\times10^{-3}\right) \tag{7}$$

Pitch of the spiral pipe	Number of pipe round	Coil diameter	Shell outer diameter
31.74 mm	3	300 mm	15.87 mm
Shell inner diameter	Outer diameter of the inner pipe		Inner diameter of the inner pipe
14.07 mm	6.35 mm		4.75 mm

Table I. Geometric properties of the present spiral heat exchanger

Distance between knots	Elements no.	Heat transfer coefficient
3	619,650	113.701
2.2	1,023,300	118.304
2	1,239,300	121.507
1.8	1,858,950	123.90

Table II. Grid independency test results

Type of nanoparticles	Density (kg/m^3)	Specific heat capacity (J/kg K)	Thermal conductivity (W/m K)
Al_2O_3	3900	880	42.34
SiO_2	2200	703	1.2
CuO	6510	535.6	18

Table III. Thermo-physical properties of nanoparticles which at this correlation the effective viscosity is defined as below equation:

$$\mu_{eff} = \mu_f \times \left(\frac{1}{1 - 34.87 \left(\frac{d_p}{d_f} \right)^{-0.3} \times \phi^{1.03}} \right) \tag{8}$$

$$d_f = \left[\frac{6M}{N \pi \rho_{f0}} \right]^{1/3} \tag{9}$$

3. Results and discussion

The SIMPLEC algorithm is used. The convergence is achieved when the normalized residuals are less than 5×10^{-13} and 5×10^{-15} for momentum and energy equations, respectively. The non-slip boundary condition is considered on the inner shell walls and all solid walls of the computational domain. The best choice for the wall function in this intense mesh near the walls is to use the improved wall function. This wall function is used for the cases in which the value of y^+ parameter near the walls is almost 1; however, more values of y^+ to about 4 to 5 are acceptable. As the values of y + are in the mentioned range, in this research, this wall function is used to model the near-wall flow.

3.1 Choosing the right model to solve the problem

By analyzing the results obtained from simulations, the most suitable model for problem-solving is selected. In Figures 3 and 4, the results of the simulation and distribution of temperature contour for the three models of standard k-ε, logic k-ε and k-ε RNG are shown for the first time (Shadloo, 2019; Hopp-Hirschler *et al.*, 2019; Sadeghi *et al.*, 2018; Hopp-Hirschler *et al.*, 2018; Toghyani *et al.*, 2019; Nasiri *et al.*, 2018; Piquet *et al.*, 2019; Shenoy *et al.*, 2019; Nguyen *et al.*, 2019; Lebon *et al.*, 2018; Sharma *et al.*, 2019; Mendez-Gonzlez *et al.*, 2018; Shadloo and Hadjadj, 2017; Rashidi *et al.*, 2017; Karimipour *et al.*, 2019; Bahrami *et al.*, 2019; Shadloo *et al.*, 2016; Jalali and Karimipour, 2019; Arabpour *et al.*, 2018a; Arabpour *et al.*, 2018b; Safaei *et al.*, 2018; Pordanjani *et al.*, 2019; Jiang *et al.*, 2019; Safaei *et al.*, 2019; Bagherzadeh *et al.*, 2019; Salimpour *et al.*, 2019; Mozaffari *et al.*, 2019; Gholamalizadeh *et al.*, 2019; Tian *et al.*, 2019; Goodarzi *et al.*, 2019; Cheloii *et al.*, 2019; Aghakhani *et al.*, 2018; Dehkordi and Abdollahi., 2018; Abdollahi *et al.*, 2018; Dehghani *et al.*, 2019; Sedeh *et al.*,

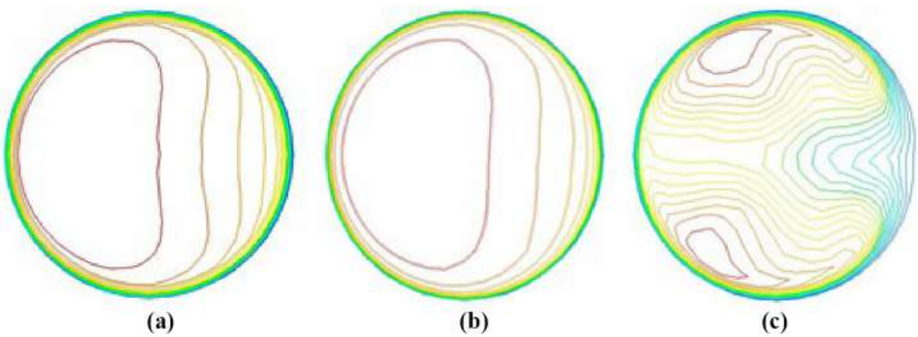

Figure 3.
Temperature contours at the inner pipe cross-section in different turbulent models including (a) Standard k-*e*, (b) k-*e* re-normalisation group (RNG) and (c) logic k-*e*

2019; Norouzipour *et al.*, 2019; Bakhshi *et al.*, 2019; Gheynani *et al.*, 2019). In all simulations, the same conditions are used (the element size of the 2 μm, which was selected as the most appropriate element size in the previous section, and the water-Al_2O_3 nanofluid with 1 per cent of nanoparticle volume fraction and Reynolds number of 1,700).

As it is visible in these two figures, the RNG model can predict the behavior of the fluid in the temperature distribution lines in an appropriate manner, assuming that the rotational flow is taken into account in its equations. In Figures 3 and 4, the RNG model, which the rotational flow is considered in its equations, has the same result as the standard model. Therefore, the RNG model can correctly predict the heat transfer properties of the fluid in the spiral double-pipe heat exchangers. These figures also demonstrate that the two standard and RNG models have a more uniform temperature distribution.

The differences in temperature in Figures 3(a), 3(b) and 3(c) are 3.9, 3.7 and 12.6, respectively, for the inner pipe side and in Figures 4(a), 4(b) and 4(c) they are 5, 3.7 and 9.3, respectively for the outer pipe side. Therefore, the RNG model with rotational flow equations shows a more uniform temperature at each cross-section than two other models. In the previous study (Ali 2014), it is reported that the prediction of the K-ε model is more accurate than the RNG turbulent model, while, according to the results obtained in this study (Figures 3 and 4), the RNG model can predict the behavior of the fluid in the temperature distribution lines better than the K-ε model, assuming that the rotational flow equations are considered. Consequently, in further numerical computations, the K-ε RNG model is used considering the rotational flow equations and element sizes of 2 μm.

3.2 Comparison of friction coefficients and pressure drop across outer tubes for different nanoparticle volume fractions

3.2.1 Friction coefficient comparison. Figures 5(a) and 5(b) imply the variations of the outer pipe friction coefficient with the Reynolds number for a different type of nanofluids at a nanoparticle volume fraction of 1 and 2 per cent, respectively, for comparison with other researchers' experimental studies. It is visible in Figure 5(a) that at Reynolds numbers less than 16,000 the differences between the present study and experimental study are higher, however, at Reynolds numbers from 16,000 to 23,000 and 23,000 to 33,000 the simulation results are in a good agreement with those of Mishka *et al.* and Ito, respectively, which proves the validity of the present numerical simulation. In Figure 5(b), also at Reynolds numbers less than 16,000 the differences between the present study and experimental studies are higher because of the type of fluid movement inside the outer pipe and generated secondary flows.

3.2.2 Pressure drop comparison. Figure 6(a), 6(b) and 6(c) display the variations of the outer pipe pressure drop with Re for various kinds of nanofluids at a concentration of 0.5, 1

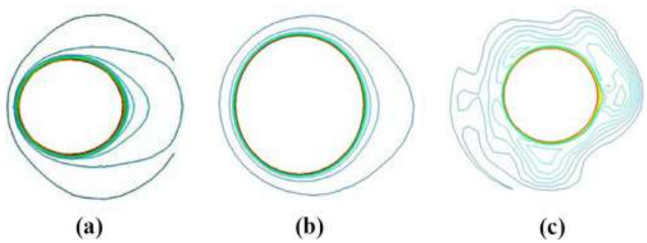

Figure 4. Temperature contours at the outer pipe cross-section in different turbulent models including (a) Standard k-*e*, (b) k-*e* RNG and (c) logic k-*e*

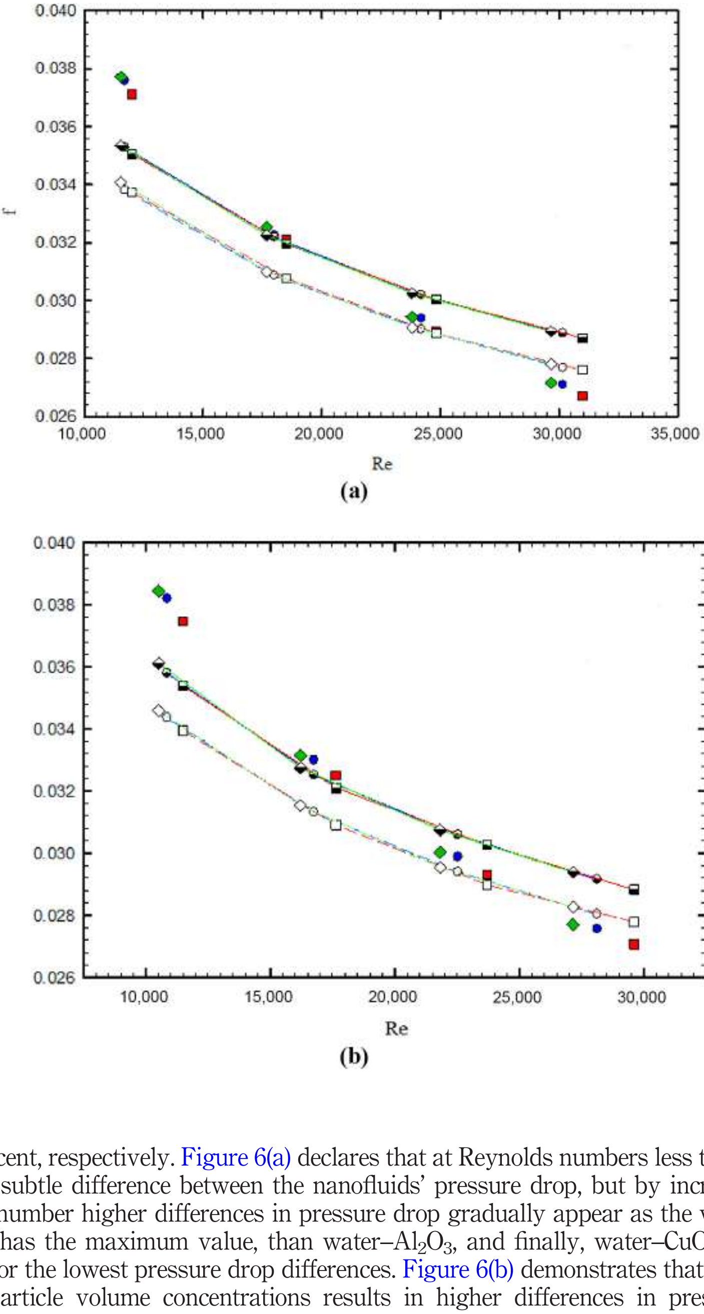

Figure 5.
Variations of the friction coefficient versus Reynolds number in outer tubes for nanofluids with nanoparticles volume fractions of (a) 1 per cent and (b) 2 per cent

and 2 per cent, respectively. Figure 6(a) declares that at Reynolds numbers less than 18,000 there is a subtle difference between the nanofluids' pressure drop, but by increasing the Reynolds number higher differences in pressure drop gradually appear as the water–SiO_2 nanofluid has the maximum value, than water–Al_2O_3, and finally, water–CuO nanofluid accounts for the lowest pressure drop differences. Figure 6(b) demonstrates that increasing the nanoparticle volume concentrations results in higher differences in pressure drop between the three nanofluids as these differences are also higher at Figure 6(c) with a higher volume fraction of nanoparticles. Hence, the water–CuO nanofluid with the lowest pressure drop is the best option between the three nanofluids as a working fluid, but the evaluation of heat transfer performance of the three nanofluids as a working fluid is of vital importance, which will be examined in the following paragraphs.

3.3 Heat transfer evaluation of the spiral double-pipe

Figures 7(a) and (b) declare the outer pipe Nusselt number versus Re for a different type of nanofluids at a nanoparticle volume fraction of 1 and 2 per cent, respectively, for comparison with other researchers' experimental studies. By increasing the nanoparticles volume fraction from 1 per cent in Figure 7(a) to 2 per cent in Figure 7(b), it is visible that the Nusselt number for water–CuO nanofluid is less than the other two nanofluids and using this type of nanofluid does not lead to the best thermal performance, while the highest values for Nusselt number accounts for water–Al_2O_3 nanofluid, then water–SiO_2 nanofluid. As the goal is to maximize the Nusselt number along with minimizing the increased pressure drop, an optimization is needed for these two parameters at the three types of nanofluids. To satisfy such a need, the genetic algorithm is used in the present study.

3.4 Finding optimal performance points using genetic algorithm

In this section, the goal is to find the points where the heat exchanger has the best performance. In fact, the optimal points for the heat exchanger are the points with the highest heat transfer coefficient and the least pressure drop. On the other hand, as shown in the hydrodynamic and thermal performance of the double-pipe spiral heat exchanger, these two parameters are similar, that is, with increasing one of them,

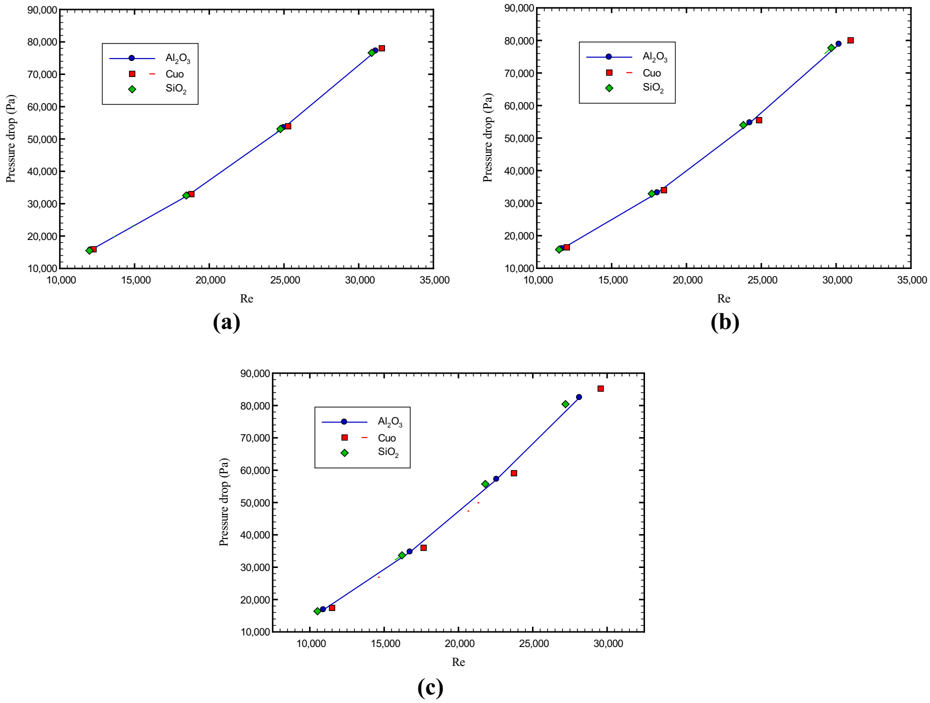

Figure 6.
Pressure drop with Reynolds number in outer tubes for nanofluids with nanoparticles volume fractions of (a) 0.5 per cent, (b) 1 per cent and (c) 2 per cent

another increase. Therefore, the multi-objective optimization problem arises. The tool used to solve the optimization problem is the multi-objective optimization toolbar of MATLAB software, which allows the use of a multi-objective genetic algorithm. Multi-objective optimization (MOO) shows to discover the optimal amount, larger than the desired target. MOO using motivation is due to optimization and also it would not need complicated equations. MOO objective function is a function of solution approach; So that there is not a unique best solution for the whole goals. The optimal set approach is named Pareto optimal method in MOO. Moreover, the genetic algorithm is a method for solving bounded and unbounded optimization problems, which acts on the basis of the principle of natural selection. In computer language, this is done by mapping the problem into a set of digital strings and changing them to get a better answer. Pareto graph obtained from optimal solutions are shown in Figure 8. In Table IV, the optimal values and the target functions values are presented as the result of the work. It can be seen that the optimal Reynolds number determines the type of nanofluid and its volume fraction, such that it can be determined by specifying the operating range of the

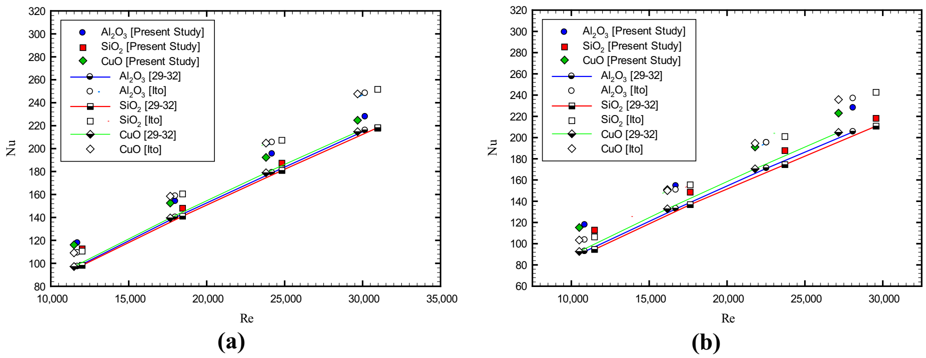

Figure 7.
Nusselt number with Reynolds number in outer tubes for nanofluids with nanoparticles volume fractions of (a) 0.5 per cent, (b) 1 per cent and (c) 2 per cent

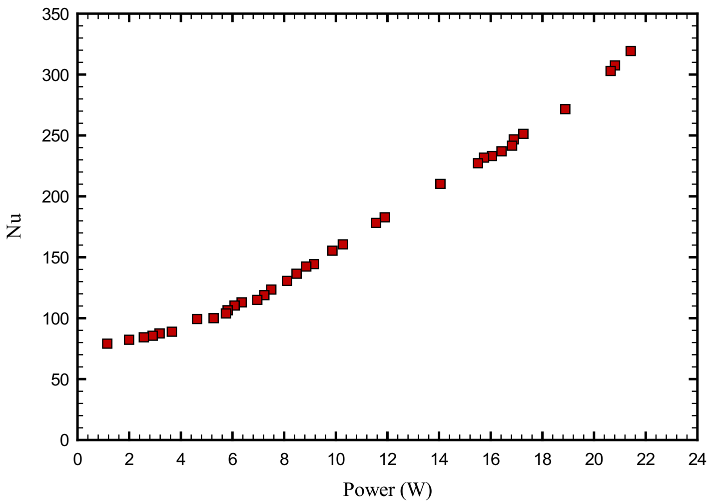

Figure 8.
The value of target functions in optimum performance points (Pareto graph)

Reynolds number	Volume fraction of nanoparticles	Type of nanoparticles	Nusselt no.	Power (W)
31,901.17	1.99	SiO_2	318.9814	21.43291
30,937.02	1.97	SiO_2	307.6649	20.83942
17,256.19	0.617	SiO_2	115.4573	6.973042
23,024.71	1.84	SiO_2	227.7134	15.56062
21,025.79	1.18	SiO_2	178.7678	11.57995
24,977.81	1.89	SiO_2	233.6169	16.08306
17,954.33	1.09	SiO_2	142.8458	8.863449
25,944.38	1.83	SiO_2	251.4614	17.27327
24,936.53	1.97	SiO_2	241.4856	16.82358
20,618.71	0.866	SiO_2	161.1074	10.2811
20,676.53	1.31	SiO_2	183.0153	11.89348
27,688.19	1.99	SiO_2	271.4293	18.93426
24,078.46	1.78	SiO_2	231.3827	15.77638
17,978.56	0.827	SiO_2	131.1974	8.119713
19,535.96	1.03	SiO_2	156.1415	9.932171
22,057.73	1.73	SiO_2	210.2056	14.07412
18,512.63	0.731	SiO_2	119.2591	7.244447
17,221.06	0.812	SiO_2	136.3113	8.505778
25,039.73	1.84	SiO_2	246.3115	16.94299
24,907.07	1.96	SiO_2	236.8019	16.44017
30,075.66	1.99	SiO_2	303.0539	20.69236
17,240.35	1.61	Al_2O_3	144.1586	9.155636
17,016.35	0.818	Al_2O_3	132.1371	8.27806
17,096.07	1.02	Al_2O_3	1,235,074	7.499914
17,376.76	0.912	Al_2O_3	99.92716	5.321148
14,807.04	1.21	Al_2O_3	110.6524	6.100972
1,595.5	0.799	Al_2O_3	103.9081	5.747926
10,551.45	0.848	CuO	79.44083	1.190658
10,784.43	1.51	CuO	84.15983	2.603882
10,935.67	1.85	CuO	88.7782	3.670601
13,020.67	1.89	CuO	106.9564	5.841581
14,437.35	1.73	CuO	113.3414	6.37848
10,907.04	1.62	CuO	87.92552	3.193572
10,724.67	1.25	CuO	82.56728	2.042345
10,524.46	1.62	CuO	85.51119	2.920706
12,423.74	1.69	CuO	99.42971	4.638544

Table IV. Related optimum Reynolds numbers and the value of target functions to the types and volume fractions of nanoparticles

nanofluid in the closed system, including a centrifuge pump and a spiral double-pipe heat exchanger, a suitable nanoparticle with the required volume concentration. At Re = 10,551 to Re = 17,220, water–Al_2O_3 is the best choice, while at Re = 17,220 to Re = 31,910, water–SiO_2 is the best option.

4. Conclusion

In this study, after presenting the results obtained from numerical simulations and selecting the k-ε RNG model with the best performance, the friction coefficient, pressure drop and heat exchanger thermal performance were investigated. The results showed that in Reynolds numbers less than 16,000, the effect of the type of nanoparticle is subtle and negligible. However, in higher Reynolds numbers, the rate of differences in pressure drop was gradually enhanced and with the augmentation in the nanoparticles' volume fractions, the differences in the pressure drop of different nanoparticles' types were seen. On the other hand, due to the interaction of the two performance parameters on each other, the genetic algorithm was used to find optimal performance conditions.

References

Abdollahi, A., Karimi Darvanjooghi, M.H., Karimipour, A. and Safaei, M.R. (2018), "Experimental study to obtain the viscosity of CuO-loaded nanofluid: effects of nanoparticles' mass fraction, temperature and basefluid's types to develop a correlation", *Meccanica*, Vol. 53 No. 15, pp. 3739-3757.

Aghakhani, S., Pordanjani, A.H., Karimipour, A., Abdollahi, A. and Afrand, M. (2018), "Numerical investigation of heat transfer in a power-law non-Newtonian fluid in a C-Shaped cavity with magnetic field effect using finite difference lattice Boltzmann method", *Computers and Fluids*, Vol. 176, pp. 51-67.

Arabpour, A., Karimipour, A. and Toghraie, D. (2018a), "The study of heat transfer and laminar flow of kerosene/multi-walled carbon nanotubes (MWCNTs) nanofluid in the microchannel heat sink with slip boundary condition", *Journal of Thermal Analysis and Calorimetry*, Vol. 131 No. 2, pp. 1553-1566.

Arabpour, A., Karimipour, A., Toghraie, D. and Akbari, O.A. (2018b), "Investigation into the effects of slip boundary condition on nanofluid flow in a double-layer microchannel", *Journal of Thermal Analysis and Calorimetry*, Vol. 131 No. 3, pp. 2975-2991.

Bagherzadeh, S.A., D'Orazio, A., Karimipour, A., Goodarzi, M. and Bach, Q.V. (2019), "A novel sensitivity analysis model of EANN for F-MWCNTs–Fe_3O_4/EG nanofluid thermal conductivity: outputs predicted analytically instead of numerically to more accuracy and less costs", *Physica A: Statistical Mechanics and Its Applications*, Vol. 521, pp. 406-415.

Bahrami, M., Akbari, M., Bagherzadeh, S.A., Karimipour, A., Afrand, M. and Goodarzi, M. (2019), "Develop 24 dissimilar ANNs by suitable architectures and training algorithms via sensitivity analysis to better statistical presentation: measure MSEs between targets and ANN for Fe–CuO/Eg–water nanofluid", *Physica A: Statistical Mechanics and Its Applications*, Vol. 519, pp. 159-168.

Bakhshi, H., Khodabandeh, E., Akbari, O., Toghraie, D., Joshaghani, M. and Rahbari, A. (2019), "Investigation of laminar fluid flow and heat transfer of nanofluid in trapezoidal microchannel with different aspect ratios", *International Journal of Numerical Methods for Heat and Fluid Flow*.

Berger, S.A., *et al.*, (1983), "Flow in curved pipes, annual review of fluid mechanics", pp. 461-512.

Cheloii, N.A., Akbari, O.A. and Toghraie, D. (2019), "Computational fluid dynamics and laminar heat transfer of water/Cu nanofluid in ribbed microchannel with a two-phase approach", *International Journal of Numerical Methods for Heat and Fluid Flow*, Vol. 29 No. 5, pp. 1563-1589.

Chingulpitak, S.S. and Wongwises, (2011), "A comparison of flow characteristics of refrigerants flowing through adiabatic straight and helical capillary tubes", *International Communications in Heat and Mass Transfer*, Vol. 38 No. 3, pp. 398-404.

Dehghani, Y., Abdollahi, A. and Karimipour, A. (2019), "Experimental investigation toward obtaining a new correlation for viscosity of WO_3 and Al_2O_3 nanoparticles-loaded nanofluid within aqueous and non-aqueous basefluids", *Journal of Thermal Analysis and Calorimetry*, Vol. 135 No. 1, pp. 713-728.

Dehkordi, B.A.F. and Abdollahi, A. (2018), "Experimental investigation toward obtaining the effect of interfacial solid-liquid interaction and basefluid type on the thermal conductivity of CuO-loaded nanofluids", *International Communications in Heat and Mass Transfer*, Vol. 97, pp. 151-162.

Dravid, A.N.K.A., Smith, E.W., Merrill, P.L.T. and Brain, (1971), "Effect of secondary fluid on laminar flow heat transfer in helically coiled tubes", *AIChE Journal*, Vol. 17 No. 5, pp. 1114-1122.

Gheynani, A.R., Akbari, O.A., Zarringhalam, M., Shabani, G.A.S., Alnaqi, A.A., Goodarzi, M. and Toghraie, D. (2019), "Investigating the effect of nanoparticles diameter on turbulent flow and heat transfer properties of non-Newtonian carboxymethyl cellulose/CuO fluid in a microtube", *International Journal of Numerical Methods for Heat and Fluid Flow*, Vol. 29 No. 5, pp. 1699-1723, available at: https://doi.org/10.1108/HFF-07-2018-0368

Gholamalizadeh, E., Pahlevanzadeh, F., Ghani, K., Karimipour, A., Nguyen, T.K. and Safaei, M.R. (2019), "Simulation of water/FMWCNT nanofluid forced convection in a microchannel filled with porous material under slip velocity and temperature jump boundary conditions", *International Journal of Numerical Methods for Heat and Fluid Flow*, available at: https://doi.org/10.1108/HFF-01-2019-0030

Goodarzi, M., Javid, S., Sajadifar, A., Nojoomizadeh, M., Motaharipour, S.H., Bach, Q.V. and Karimipour, A. (2019), "Slip velocity and temperature jump of a non-Newtonian nanofluid, aqueous solution of Carboxy-methyl cellulose/aluminum oxide nanoparticles, through a microtube", *International Journal of Numerical Methods for Heat and Fluid Flow*, Vol. 29 No. 5, pp. 1606-1628, available at: https://doi.org/10.1108/HFF-05-2018-0192

Hopp-Hirschler, M.M.S., Shadloo, U. and Nieken, (2019), "Viscous fingering phenomena in the early stage of polymer membrane formation", *Journal of Fluid Mechanics*, Vol. 864, pp. 97-140.

Hopp-Hirschler, M., Shadloo, M.S. and Nieken, U. (2018), "A smoothed particle hydrodynamics approach for thermo-capillary flows", *Computers and Fluids*, Vol. 176, pp. 1-19.

Jalali, E. and Karimipour, A. (2019), "Simulation the effects of cross-flow injection on the slip velocity and temperature domain of a nanofluid flow inside a microchannel", *International Journal of Numerical Methods for Heat and Fluid Flow*, Vol. 29 No. 5, pp. 1546-1562.

Jiang, Y., Bahrami, M., Bagherzadeh, S.A., Abdollahi, A., Sulgani, M.T., Karimipour, A., Goodarzi, M. and Bach, Q.V. (2019), "Propose a new approach of fuzzy lookup table method to predict Al_2O_3/deionized water nanofluid thermal conductivity based on achieved empirical data", *Physica A: Statistical Mechanics and Its Applications*, Vol. 527, p. 121177.

Jung-Yang (2012), "Heat transfer characteristics of a helical heat exchanger", *Applied Thermal Engineering*, pp. 114-120.

Kahani, M., Zeinali Heris, S. and Mousavi, S.M. (2013), "Effects of curvature ratio and coil pitch spacing on heat transfer performance of Al2O3-Water nanofluid laminar flow through helical coils", *Journal of Dispersion Science and Technology*, Vol. 34 No. 12, pp. 1704-1712.

Kalteh, M., Abbassi, A., Saffar-Avval, M. and Harting, J. (2011), "Eulerian–Eulerian two-phase numerical simulation of nanofluid laminar forced convection in a micro channel", *International Journal of Heat and Fluid Flow*, Vol. 32 No. 1, pp. 107-116.

Karimipour, A., Bagherzadeh, S.A., Taghipour, A., Abdollahi, A. and Safaei, M.R. (2019), "A novel nonlinear regression model of SVR as a substitute for ANN to predict conductivity of MWCNT-CuO/water hybrid nanofluid based on empirical data", *Physica A: Statistical Mechanics and Its Applications*, Vol. 521, pp. 89-97.

Kurnia, J.C., Sasmito, A.P. and Mujumdar, A.S. (2011a), "Evaluation of heat transfer performance of helical coils of noncircular tubes", *Journal of Zhejiang University-Science A*, Vol. 12 No. 1, pp. 63-70.

Kurnia, J.C., Sasmito, A.P. and Mujumdar, A.S. (2011b), "Numerical investigation of laminar heat transfer performance of various cooling channel designs", *Applied Thermal Engineering*, Vol. 31 Nos. 6/7, pp. 1293-1304.

Lebon, B., Nguyen, M.Q., Peixinho, J., Shadloo, M.S. and Hadjadj, A. (2018), "A new mechanism for the periodic bursting of the recirculation region of the flow through a sudden expansion in a circular pipe", *Physics of Fluids*, Vol. 30 No. 3, p. 031701.

Maakoul, A.E.A., Laknizi, S., Saadeddine, A.B., Abdellah, M., Meziane, M.E. and Metoui, (2017), "Numerical design and investigation of heat transfer enhancement and performance for an annulus with continuous helical baffles in a double-pipe heat exchanger", *Energy Conversion and Management*, Vol. 133, pp. 76-86.

Mendez-Gonzlez, M., Shadloo, M.S., Hadjadj, A. and Ducoin, A. (2018), "Boundary layer transition over a concave plate caused by centrifugal instabilities", *Computers and Fluids*, Vol. 171, pp. 135-153.

Mozaffari, M., D'Orazio, A., Karimipour, A., Abdollahi, A. and Safaei, M.R. (2019), "Lattice Boltzmann method to simulate convection heat transfer in a microchannel under heat flux: gravity and inclination angle on slip-velocity", *International Journal of Numerical Methods for Heat and Fluid Flow*.

Naphon, P. and Wongwises, S. (2006), "A review of flow and heat transfer characteristics in curved tubes", *Renewable and Sustainable Energy Reviews*, Vol. 10 No. 5, pp. 463-490.

Naphon, P.S. and Wongwises, (2002), "An experimental study on the in-tube heat transfer coefficients in Aspiral-coil heat exchanger", *International Communications in Heat and Mass Transfer*, Vol. 29 No. 6, pp. 797-809.

Nasiri, H., Jamalabadi, M.Y.A., Sadeghi, R., Safaei, M.R. and Shadloo, M.S. (2018), "A smoothed particle hydrodynamics approach for numerical simulation of Nano-Fluid flows: Application to forced convection heat transfer over a horizontal cylinder", *Journal of Thermal Analysis and Calorimetry*, doi: 10.1007/s10973-018-7022-4.

Nguyen, M.Q., Shadloo, M.S., Hadjadj, A., Lebon, B. and Peixinho, J. (2019), "Perturbation threshold and hysteresis associated with the transition to turbulence in sudden expansion pipe flow", *International Journal of Heat and Fluid Flow*, Vol. 76, pp. 187-196.

Norouzipour, A., Abdollahi, A. and Afrand, M. (2019), "Experimental study of the optimum size of silica nanoparticles on the pool boiling heat transfer coefficient of silicon oxide/deionized water nanofluid", *Powder Technology*, Vol. 345, pp. 728-738.

Paisarn, N. and Jamnean, S. (2006), "*Effect of Curvature Ratios on the Heat Transfer and Flow Developments in the Horizontal Spirally Coiled Tubes*, Department of Mechanical Engineering,

Pawar, S.S. (2013), *Experimental Thermal and Fluid Science*, pp. 792-804.

Piquet, A., Zebiri, B., Hadjadj, A. and Shadloo, M.S. (2019), "A parallel High-Order compressible flows solver with a domain decomposition method in the generalized curvilinear coordinates system", *International Journal of Numerical Methods for Heat and Fluid Flow*, doi: 10.1108/HFF-01-2019-0048.

Pordanjani, A.H., Aghakhani, S., Karimipour, A., Afrand, M. and Goodarzi, M. (2019), "Investigation of free convection heat transfer and entropy generation of nanofluid flow inside a cavity affected by magnetic field and thermal radiation", *Journal of Thermal Analysis and Calorimetry*, pp. 1-23.

Rashidi, M.M., Nasiri, M., Shadloo, M.S. and Yang, Z. (2017), "Entropy generation in a circular tube heat exchanger using nanofluids: effects of different modeling approaches", *Heat Transfer Engineering*, Vol. 38 No. 9, pp. 853-866.

Sadeghi, R., Shadloo, M.S., Hopp-Hirschler, M., Hadjadj, A. and Nieken, U. (2018), "Three-dimensional lattice Boltzmann simulations of high density ratio two-phase flows in porous media", *Computers and Mathematics with Applications*, Vol. 75, pp. 2445-2465.

Saeedan, M., Solaimany Nazar, A.R., Abbasi, Y. and Karimi, R. (2016), "CFD investigation and neutral network modeling of heat transfer and pressure drop of nanofluids in double pipe helically baffled heat exchanger with a 3-D fined tube", *Chemical Engineering Research and Design*, Vol. 100, pp. 721-729.

Safaei, M.R., Karimipour, A., Abdollahi, A. and Nguyen, T.K. (2018), "The investigation of thermal radiation and free convection heat transfer mechanisms of nanofluid inside a shallow cavity by lattice Boltzmann method", *Physica A: Statistical Mechanics and Its Applications*, Vol. 509, pp. 515-535.

Safaei, M.R., Ranjbarzadeh, R., Hajizadeh, A., Bahiraei, M., Afrand, M. and Karimipour, A. (2019), "Effects of cobalt ferrite coated with silica nanocomposite on the thermal conductivity of an antifreeze: new nanofluid for refrigeration condensers", *International Journal of Refrigeration*, Vol. 102, pp. 86-95.

Salimpour, M.R. (2009), "Heat transfer coefficients of shell and coiled tube heat exchangers", *Experimental Thermal and Fluid Science*, Vol. 33 No. 2, pp. 203-207.

Salimpour, M.R., Karimi Darvanjooghi, M.H., Abdollahi, A., Karimipour, A. and Goodarzi, M. (2019), "Providing a model for csf according to Pool boiling convection heat transfer of water/ferrous oxide nanofluid using sensitivity analysis", *International Journal of Numerical Methods for Heat and Fluid Flow*.

Sedeh, R.N., Abdollahi, A. and Karimipour, A. (2019), "Experimental investigation toward obtaining nanoparticles' surficial interaction with basefluid components based on measuring thermal conductivity of nanofluids", *International Communications in Heat and Mass Transfer*, Vol. 103, pp. 72-82.

Shadloo, M.S. (2019), "Numerical simulation of compressible flows by lattice Boltzmann method", *Numerical Heat Transfer, Part A*, Vol. 75 No. 3, pp. 167-182.

Shadloo, M.S. and Hadjadj, A. (2017), "Laminar-turbulent transition in supersonic boundary layers with surface heat transfer: a numerical study", *Numerical Heat Transfer, Part A: Applications*, Vol. 72 No. 1, pp. 40-53.

Shadloo, M.S., Oger, G. and Le Touze, D. (2016), "Smoothed particle hydrodynamics method for fluid flows, towards industrial applications: motivations, current state, and challenges", *Computers and Fluids*, Vol. 136, pp. 11-34.

Sharma, S., Shadloo, M.S., Hadjadj, A. and Kloker, M.J. (2019), "Control of oblique-type breakdown in a supersonic boundary layer employing streaks", *Journal of Fluid Mechanics*, Vol. 873, doi: 10.1017/jfm.2019.435.

Shenoy, D.V., Shadloo, M.S., Hadjadj, A. and Peixinho, J. (2019), "Direct numerical simulations of laminar and transitional flows in diverging pipes", *International Journal of Numerical Methods for Heat and Fluid Flow*, doi: 10.1108/HFF-02-2019-0111.

Tian, Z., Bagherzadeh, S.A., Ghani, K., Karimipour, A., Abdollahi, A., Bahrami, M. and Safaei, M.R. (2019), "Nonlinear function estimation fuzzy system (NFEFS) as a novel statistical approach to estimate nanofluids' thermal conductivity according to empirical data", *International Journal of Numerical Methods for Heat and Fluid Flow*.

Toghyani, S., Afshari, E., Baniasadi, E. and Shadloo, M.S. (2019), "Energy and exergy analyses of a nanofluid based solar cooling and hydrogen production combined system", *Renewable Energy*, Vol. 141, pp. 1013-1025.

Zhao, Z.X., Wang, D., Che, Z. and Cao, (2011), "Numerical studies on flow and heat transfer in membrane helical-coil heat exchanger and membrane serpentine-tube heat exchanger", *International Communications in Heat and Mass Transfer*, Vol. 38 No. 9, pp. 1189-1194.

Corresponding author
Marjan Goodarzi can be contacted at: marjan.goodarzi@tdtu.edu.vn